SCIENTIFIC REPORTS

OPEN

SUBJECT AREAS:
MOLECULAR SELF-ASSEMBLY
TISSUE ENGINEERING AND REGENERATIVE MEDICINE

Received
4 June 2014

Accepted
9 October 2014

Published
11 November 2014

Correspondence and requests for materials should be addressed to K.S.I. (swaminatha.iyer@uwa.edu.au)

* These authors contributed equally to this work.

Designer self-assembling hydrogel scaffolds can impact skin cell proliferation and migration

Michael Bradshaw[1]*, Diwei Ho[1]*, Mark W. Fear[2], Fabrizio Gelain[3,4], Fiona M. Wood[2,5] & K. Swaminathan Iyer[1]

[1]School of Chemistry and Biochemistry, M313, The University of Western Australia, 35 Stirling Highway, Crawley, WA, 6009 (Australia), [2]Fiona Wood Foundation and Burn Injury Research Unit, M318, The University of Western Australia, 35 Stirling Highway, Crawley, WA, 6009 (Australia), [3]Center for Nanomedicine and Tissue Engineering, CNTE - 4th floor Pad. Mariani, A.O., Ospedale Niguarda Ca' Granda, Piazza dell'Ospedale Maggiore 3, Milan, 20162 (Italy), [4]IRCCS Casa Sollievo della Sofferenza Opera di San Pio da Pietrelcina, San Giovanni Rotondo 71013 (Italy), [5]Burns Service of Western Australia, Royal Perth and Princess Margaret Hospitals, WA, 6000 (Australia).

There is a need to develop economical, efficient and widely available therapeutic approaches to enhance the rate of skin wound healing. The optimal outcome of wound healing is restoration to the pre-wound quality of health. In this study we investigate the cellular response to biological stimuli using functionalized nanofibers from the self-assembling peptide, RADA16. We demonstrate that adding different functional motifs to the RADA16 base peptide can influence the rate of proliferation and migration of keratinocytes and dermal fibroblasts. Relative to unmodified RADA16; the Collagen I motif significantly promotes cell migration, and reduces proliferation.

Skin, the largest organ of the human body, provides an essential protective barrier and has several homeostatic/sensory functions vital to health. Functional recovery post-injury remains a principal goal of tissue engineering research. Although the skin has the ability to self-heal and regenerate in minor injuries such as cuts and abrasions, in all but trivial injuries the capacity to repair without scarring is overwhelmed, resulting in extensive scarring[1]. A breach in skin integrity is associated with the potential for invasion of microorganisms; resulting in infection, a significant cause of morbidity and mortality. In instances where a large surface area of skin is damaged, such as with severe burns and other traumatic injuries, fluid loss through the skin can lead to dehydration and consequently, life-threatening hypovolemic shock[2].

Whenever available, the skin replacement material of choice is the patients' own (autologous) skin. In smaller injuries, this can be accomplished by split-thickness skin autografts (STG)[3]. The donor site from the STG heals like a superficial partial thickness wound, and once healed, can be used for further STG re-harvesting[4]. Nevertheless, donor areas are limited in extensive injuries and scarring is significant due to the lack of harvested dermis. Autografts can be meshed, uniformly perforated and stretched to cover greater areas of the wound, but the cosmetic and functional outcomes are inferior to standard STG application[5,6]. A more complete reconstruction can be obtained with full thickness skin grafts (epidermis and whole dermis), which are limited in dimension and can only be harvested from a few areas. Donor-site morbidity and technical difficulties limit the usefulness of these types of grafts. Furthermore, severely injured patients invariably lack sufficient donor sites for skin grafts. More importantly, the application of STGs to full-thickness wounds usually leads to scar formation which is often vulnerable and unstable, frequently resulting in severe debilitating contractures due to the lack of dermal support[7]. Such limitations of this treatment have driven the search for synthetic scaffolds to resurface the wound and facilitate rapid healing.

Cell migration, differentiation, and survival are important parameters that determine the outcome of a successful regeneration platform. These in turn rely on the ability of cells to coordinate diverse inputs from cytokines, growth factors, and extracellular matrix (ECM) molecules. Amongst these factors, the communication of cells with the ECM is a dominating factor[8]. This is complicated by the fact that remodeling of the ECM can also occur under normal physiological conditions, as a result of tissue injury, or in various pathological conditions. ECM remodeling leads to alterations in ECM organization and composition that can alter many aspects of cell behavior, including cell migration. One of the most well documented design constraints in the development of synthetic

scaffolds is the ability to mimic the dimensions of the ECM to support cell adhesion and migration[9]. Polymer based synthetic scaffold materials such as poly (L)-lactic acid and poly-glycolic acid are two of the most commonly explored materials[10–12] with predictable and reproducible mechanical and physical properties (tensile strength, pore size, etc.)[6]. There are two major drawbacks with this approach; firstly, synthetic materials generally elicit a foreign immune response, specifically, a fibrous tissue deposition leading to formation of keloid scars[13]. Secondly, these scaffolds suffer inherently by their inability to mimic the dynamic nature of the ECM remodeling process - both in composition and morphology.

The aforementioned issues can be overcome using self-assembling peptides (SAP), where the final scaffold structure is a consequence of specific, local interactions among the basic components that form the scaffold[14]. SAP nanofiber scaffolds are synthetic scaffolds formed by the assembly of ionic, self-complementary peptides. The alternating positive and negative L-amino acids within the peptides form highly hydrated scaffolds in the presence of neutral pH solutions and physiological concentrations of salts[15]. These salts can typically be found in bodily fluids (e.g. blood serum) or tissue culture media. The most extensively studied SAP is RADA16 (RADARADARADARADA). RADA16 consists of 16 alternating hydrophobic and hydrophilic amino acids, forming an extremely stable β-sheet structure and self-assembles into nanofibers to produce a scaffold hydrogel[16]. The periodically repeating β-sheets of ionic peptides contain charged residues on one side and hydrophobic side chains on the other; resulting in interwoven nanofibers. Individual hydrated fibers are ≈10 nm in diameter and range from a few hundred nanometers to a few microns in length[17]. RADA16 is easy to modify at the single amino acid level without altering its ability to self-assemble and adding biologically active motifs to the peptide can give the scaffold the ability to influence cellular behavior.

Three peptides were the focus of the current study. RADA16 (RADARADARADARADA), RADA16 with a fibronectin motif (RADA16-GG-RGDS) and RADA16 with a collagen type I motif (RADA16-GG-FPGERGVEGPGP). Two glycine residues (GG) are added to ensure exposure and flexibility of the functional motifs. For the sake of brevity in this report, the collagen type I motif will be abbreviated to FPG and the fibronectin motif will be abbreviated to RGD. Using these peptides, we will explore the ability of functional motifs on self-assembling peptide scaffolds to influence the proliferation and migration of fibroblasts and keratinocytes. Understanding the influences of these motifs on cell interactions with the peptides will aid in the design of scaffolds that not only mimic the ECM morphology but also incorporate the need to address the dynamic biochemical influence of the ECM during the regeneration process. Indeed, functionalized RADA16 with designer motifs has been shown to be more effective than non-functionalized RADA16 for promoting cell survival, attachment and growth[18]. Further to this, functionalization of RADA16 with a RGD motif was demonstrated to significantly increase osteoblast proliferation[19].

Results

RADA16 (1% w/v) was previously tested for the treatment of second degree burns in rats and compared against collagen type I, chitosan and poly lactic acid, with RADA16 showing the most significant improvement in wound healing outcomes[20]. In the current study we initially examined whether the addition of functional motifs to the RADA16 peptide would affect the morphology of the gels. Scanning electron microscopy (SEM) was performed on all three gels at 1% w/v (Figure 1a–c). The three gels demonstrated similar morphology with densely packed fibers in random orientations. The diameters of the nanofibers were ≈10–20 nm, in accordance with previously reported values[14].

To determine the viability of fibroblasts (NIH-3T3) and keratinocytes (HaCaT) on the SAPs, a MTS cell proliferation assay was performed in triplicate over 72 hours (Figure 1d). It is noteworthy that cell only controls were excluded from significance testing due to the fact that they were grown on a 2D surface, rather than a 3D hydrogel. Data from the cell only controls is included for completeness, but should not be compared with the data obtained from the functionalized RADA16 gels. It is evident that RADA16-FPG inhibited cell proliferation significantly for fibroblasts and moderately for keratinocytes when compared to RADA16 and RADA16-RGD scaffolds at 72 hours. Because of HaCaT keratinocytes slower growth rate, a significant difference in proliferation was not seen over the time period studied, but a trend towards lesser proliferation in FPG and RGD scaffolds was still observable.

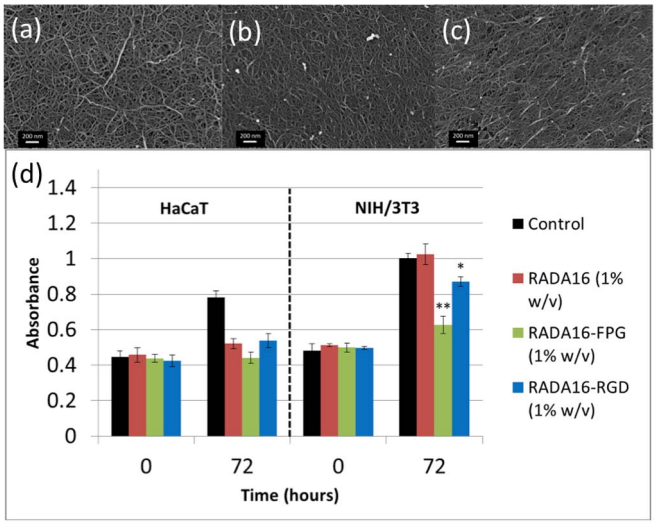

Figure 1 | Scanning electron microscopy and cell proliferation on 1w/v% RADA16 scaffolds. SEM of (a) RADA16, (b) RADA16-FPG and (c) RADA16-RGD. Scale bars are 200 nm. (d) Cell viability data for keratinocytes/fibroblasts on the three 1% w/v RADA16 scaffolds and cell-only control after 0 and 72 hours of incubation. Cell viability was tested with MTS assays. Experiments were done in triplicate. Significance was tested against RADA16 for both cell types (*$p < 0.05$; **$p < 0.01$).

To further investigate why the addition of the functional motifs reduced fibroblast proliferation, we performed live cell imaging to observe the cells on the scaffolds. We expected the functionalized scaffolds, in particular RADA16-FPG to enhance the migration rates over non-functionalized RADA16 because of the suppression of the proliferative phenotype that we demonstrated with the MTS experiments[21]. Traditionally cell migration is quantified using scratch assays[22], Teflon fence[23] or Boyden chambers[24]. Both the scratch and Teflon fence assay are limited to studying cell migration on rigid 2D surfaces and are not suitable for a hydrogel substrate such as RADA16. The Boyden chamber is commonly used to study 3D migration, but is not useful for quantifying cell migration on a hydrogel scaffold in real time. We used time-lapse, differential interference contrast (DIC) microscopy with a live cell chamber and captured images every 6 minutes for 12 hours. Using these images, the path and distance of each individual cell was tracked (Figure 2a–c). The cells appeared rounded on the gels and were highly motile during the period observed. This is to be expected with these types of cells on soft hydrogels[25–27]. Cell migration was quantified frame-by-frame using the image analysis software, Fiji[28] (videos of the time-lapse microscopy can be found in the supporting information). It was apparent that RADA16-FPG significantly enhanced cell migration of fibroblasts compared to RADA16 and RADA16-RGD (Figure 2d). There appeared to be a similar trend with the keratinocytes, but due to their non-migratory nature and the fact that cells could only be tracked in two dimensions over the gel, there was no significant difference

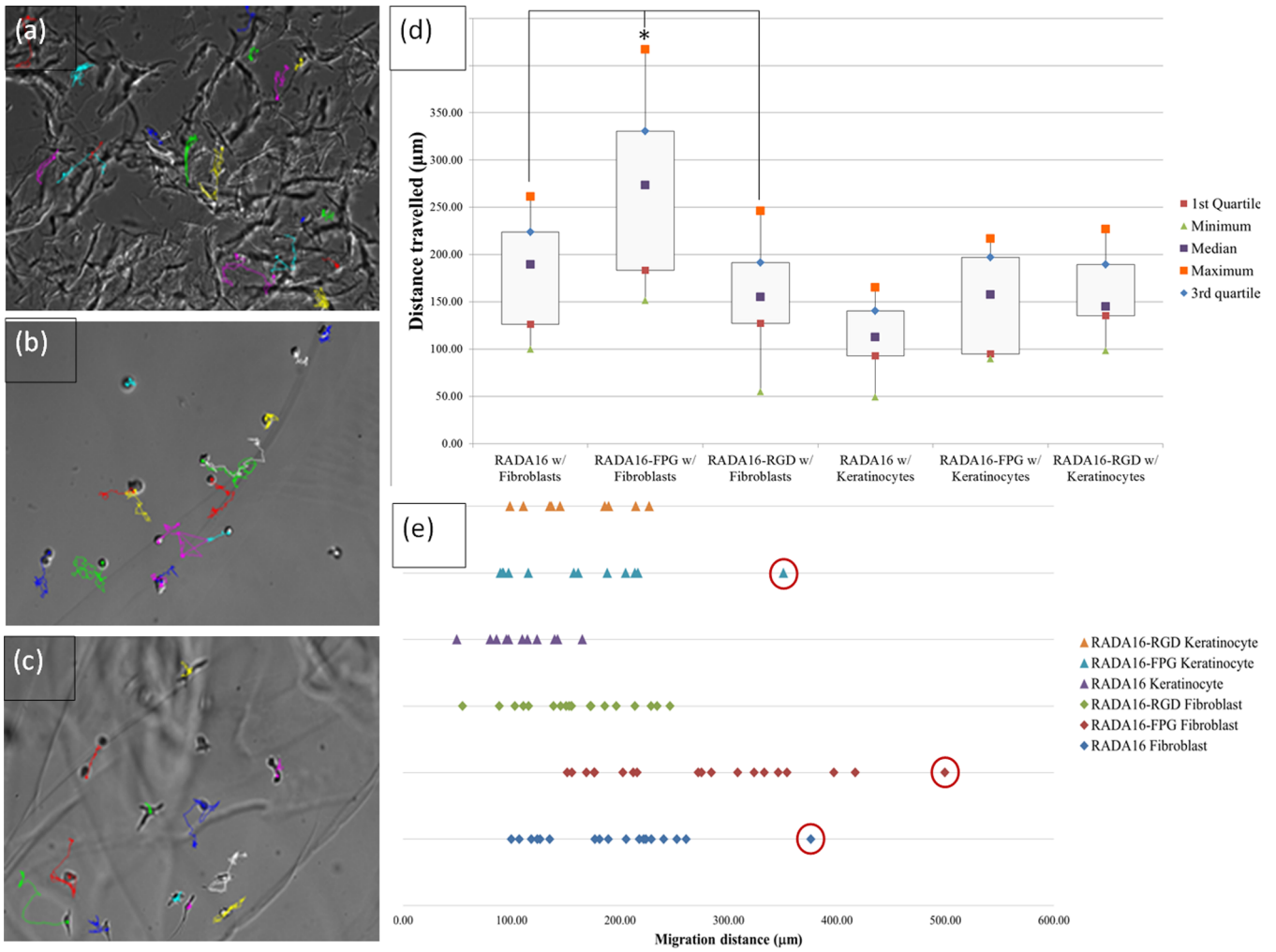

Figure 2 | Live cell tracking migration assay on RADA16 scaffolds. (a) Representative differential interference contrast (DIC) optical microscopy still images taken from the live cell tracking at the 12 hour time point for (a) RADA16, (b) RADA16-FPG and (c) RADA16-RGD. The cells tracked are marked and their paths tracked as trailing lines. (Full set of images and live cell videos in the supplementary information S3.) (d) Box plot summary of fibroblast and keratinocyte migration on all three scaffolds over a period of 12 hours and (e) point distribution with outliers circled. Outliers were excluded from data analysis (*$p < 0.05$ one way ANOVA with a Bonferroni means comparison).

between the functionalized hydrogels. The fibronectin motif (RGD) had no significant effect on either cell type's migration.

Discussion

At the wound site, a host of biomolecules interact with each other to form the provisional matrix; a temporary form of ECM that acts as a scaffold from which the dermis is reconstructed[29]. The provisional matrix is mainly made up of fibrin, fibronectin and hyaluronic acid[30]. The presence of fibronectin promotes the adhesion, migration and chemotaxis of neutrophils, macrophages, endothelial cells, keratinocytes and fibroblasts[16]. There are several different stimuli for cells in the wound to migrate; firstly, the loss of basal cell–cell contact starts the basal keratinocyte's migration and growth factors that target epithelial cells are released from the wound to stimulate migration. Basal cells have a tendency to stay on the basement membrane if they are in contact with proteins such as laminin and collagen type IV, but when they come in contact with proteins found in the wound (e.g. fibronectin and collagen type I), they are encouraged to migrate[31].

Granulation tissue, named for its granular appearance due to new capillaries, is formed approximately four days after injury[30]. The blood vessels supply the immediate area with oxygen and nutrients, supporting the fibroblasts as they replace the provisional matrix with a collagen-rich matrix[30]. In the granulation tissue, collagen type I is the dominant ECM fiber. It provides form and tensile strength to the tissue. Non-collagenous glycoproteins such as fibronectin and laminin organize the extracellular matrix and facilitate cell-matrix interactions[32]. Collagen is a key connective tissue protein in all mammals and has been used as a wound management material in burns and partial thickness wounds[33].

Migrating keratinocytes and fibroblasts use a provisional matrix in the wound bed that is rich in fibrin, fibronectin and hyaluronic acid[34]. The proliferative and migratory rates of fibroblasts and keratinocytes can be attributed to the expression of integrins – cell surface, matrix adhesion and signaling receptors that recognize the ECM motifs[35]. During different phases of wound healing, the integrin receptor profile changes, altering adhesion affinity to different types of ECM motifs and influencing cell behavior[36]. The phenotypes induced are generally polarized towards one of two options - migratory or proliferative[37]. When cells adopt a migratory phenotype, ECM remodeling enzymes called matrix metalloproteinases are activated and proliferative abilities are suppressed[38]. The RGD sequence (Arg-Gly-Asp) is a cell attachment site present in ECM proteins recognized by almost half of the known integrin receptors. The integrin binding activity of the ECM can be reproduced by short synthetic peptides containing the RGD sequence, e.g. fibronectin (RGDS)[39]. Type I and III collagen are the main, fiber forming collagens in

normal human dermis and they constitute the bulk of large collagen fibers. Type I collagen comprises about 80% of dermal collagen and plays a major role in providing tensile strength to skin. In the initial phase of wound healing, type III collagen and fibronectin are deposited. Type III collagen is eventually replaced by type I collagen during the later stages of wound healing[34]. Type I collagen has been shown to dramatically promote keratinocyte migration *in vitro*[40].

In order to better understand the cell - nanofiber interactions, we analyzed the samples using SEM. Samples were fixed and processed at 0 and 72 hours after seeding the cells on the nanoscaffolds. Both fibroblasts and keratinocytes appear to be migrating into the nanoscaffolds, as evidenced by the appearance of 'pits' after 72 hours (Figure 3). No other such pits were found in t = 0 samples and where cells were absent in the t = 72 samples. Under the SEM, most cells were seen to have spherical morphologies; this is most likely due to the glutaraldehyde fixing/ethanol dehydration and CO_2 critical point drying steps, rendering the cell culture environment unfavorable and causing the cells to retract their micro-extensions[41]. Furthermore, it appeared that the fibroblasts migrated deeper and became more settled into the nanoscaffolds as compared with the keratinocytes. This observation was corroborated by our proliferation and migration data where keratinocytes were slower to grow and migrate.

We demonstrate that the design of a regenerative scaffold should take into account not only the morphology but also the ability to mimic the dynamic ECM at the injury site. Using keratinocytes and fibroblasts as a model system we show that incorporating peptide motifs as cues in a self-assembling peptide scaffold can serve as an attractive ECM mimic. We have demonstrated this through the use of three types of SAP (RADA16, RADA16-FPG and RADA16-RGD).

In summary, we showed that cellular migration can be significantly increased using a FPG peptide motifs and proliferation can be decreased. For the best wound healing outcome, an enhanced cellular migration is extremely important, more so than proliferation in that cells must migrate through the wound to achieve wound closure and full re-epithelialization. We envision that a bimodal or gradient system would be used in the future, with migratory motifs promoting cell migration into a region with proliferation inducing motifs, e.g. a shell of RADA16-FPG surrounding a core structure of RADA16.

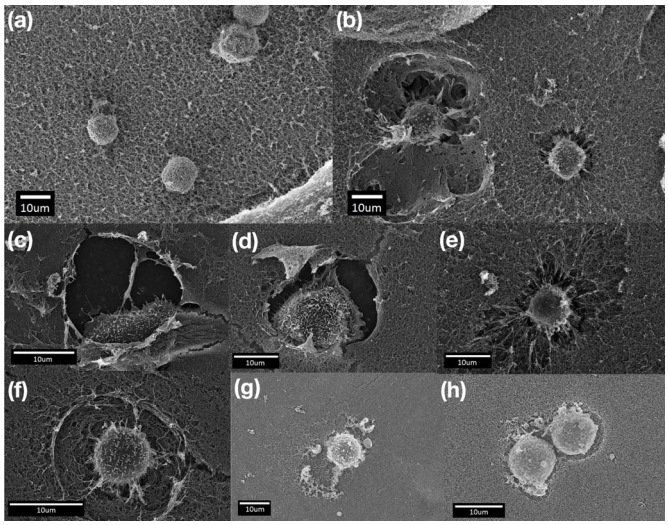

Figure 3 | Scanning electron microscopy of cell interactions with RADA16 scaffolds. (a) Fibroblasts on RADA16 1% w/v after (a) 0 and (b) 72 hours (see supplementary information S1 and S2 for keratinocytes and fibroblasts on all three SAP nanofiber scaffolds after 0 and 72 hours of seeding). (c–e) Fibroblasts and (f–h) keratinocytes seeded on RADA16, RADA16-FPG and RADA16-RGD scaffolds.

Specific biological motifs can have a significant effect on cell behavior as we have demonstrated with our proliferation and migration data. The major impact of this work aids the understanding of how using functionalized motifs can be incorporated in the final design of a regenerative platform to improve the efficacy in cutaneous wound healing.

Methods

Cell culture. HaCaT (immortalized human keratinocytes) and NIH/3T3 (mouse embryonic fibroblasts) cell lines were used. Both cell lines were cultured in Dulbecco's Modified Eagle's Medium (DMEM/F12 - GlutaMAX; Invitrogen Gibco) supplemented with 10% fetal bovine serum (FBS; Invitrogen Gibco) and 1% penicillin/streptomycin (P/S; Invitrogen Gibco). The cells were incubated at 37°C and in an atmosphere of 5% CO_2. Cells were passaged at ~80% confluency and seeded in 75 cm^2 tissue culture flasks (Greiner Bio-One, cat. No. 658175). All procedures involving cell-handling were performed under standard sterile conditions.

Preparation of peptide solutions. Lyophilized RADA16, RADA16-FPG and RADA16-RGD were custom synthesized and purchased from China Peptides (Purity > 90%, Shanghai, China). All peptides used have the following modifications: acetylation (N-terminal) and amidation (C-terminal). Motifs were directly synthesized onto the C-terminal end of RADA16 using solid-phase peptide synthesis. To ensure the correct exposure and flexibility of the functional motif, two glycine residues are inserted between the functional motif and RADA16. The SAPs were dissolved in MilliQ water at 1% (w/v, 10 mg mL^{-1}) and sonicated for 20 minutes (Unisonics, model FXP10DH). The solutions were sterilized under UV for 1 hour and stored at −20°C. Solutions were sonicated for 20 minutes prior to use.

Formation of SAP nanoscaffolds. 50 μL of SAP solutions at 1% w/v concentration was pipetted onto the substrate and 50 μL of DMEM mixture was added to initiate gelation (formation of SAP nanoscaffolds). The substrate used was dependent on the assay. For the proliferation assays, plastic 96 well plates were used. For the live-cell imaging, specifically designed dishes were used with a No. 1.5 glass coverslip (10 mm microwell with 0.16–0.19 mm thickness) inside a plastic 35 mm petri dish. Samples were covered and left to stand for 10 minutes in standard room conditions to ensure complete gelation. An additional 100 μL of DMEM mixture was added on top of the sample following gelation. This additional volume of media was removed and changed twice with an equal volume of DMEM mixture to equilibrate the pH.

Scanning electron microscopy of SAP nanoscaffolds and cell. Poly-L-lysine (1 mg mL^{-1}; Sigma-Aldrich) coated glass coverslips (10 mm diameter; ProSciTech) were prepared by adding 50 μL of poly-L-lysine on them and leaving to dry overnight. The resultant monolayer of poly-L-lysine significantly reduces the detachment of SAP nanoscaffolds from the coverslip during the pH equilibration steps. Only the samples prepared for SEM imaging had poly-l-lysine added to the coverslips. SAP nanoscaffolds were prepared on the coverslips. For samples with cells, 100 μL of fibroblasts and keratinocytes (1.5×10^4 cells mL^{-1}) were seeded separately on the pH equilibrated SAP nanoscaffolds and left to incubate (37°C/5% CO_2) for 72 hours.

In preparation for SEM imaging, samples were immersed in 2.5% glutaraldehyde and were kept at 4°C for two hours. Following which, the samples were washed with phosphate buffered saline (PBS; pH 7.4) and immersed in increasing concentrations of ethanol (50%, 70%, 90% and twice in absolute 'dry' ethanol). In between each immersion, the samples were dehydrated in a specialized microwave (PELCO, BioWave 34700 Laboratory Microwave System). Critical point drying (which replaces the ethanol in the sample with supercritical CO_2) was performed to complete the dehydration process.

The processed coverslips were mounted on SEM mounts (ProSciTech, cat. No. G040) with carbon tabs. As the samples were non-conductive, they were coated with 3 nm of platinum before being visualized under the scanning electron microscope (SEM; Zeiss 1555 VP-FESEM). The SEM images were taken using the in-lens detector at 4–5 mm working distance, 30 μm aperture and accelerating voltage at 5 kV. Images were analyzed with the image analysis software Fiji (ImageJ).

Statistical Analysis. The data was checked to be normally distributed and the Brown-Forsythe test for equal variance was applied. The data conformed to all requirements necessary for the following statistical tests. For the statistical analysis performed on both the proliferation and the migration data, a one way ANOVA was used at a familywise significance threshold of 0.05 with a Bonferroni correction for multiple comparisons. The standard error of the mean was plotted as error bars in all cases.

Cell proliferation assays (MTS assays). The MTS assay indirectly measures cell population through the reduction of a tetrazolium compound to produce a colored formazan product, measured at an absorbance of 490 nm. Cellular metabolism induces a reduction of the tetrazolium compound, so the quantity of the formazan product (and therefore the optical density of the solution) is proportional to the level of cellular proliferation in the sample. It is commonly used as a measure of cell viability and cytotoxicity of medicinal agents[42,43].

Separate 96-well plates (Greiner Bio-One) were prepared for each sampling time point (0, 24, 48, 72 hours). SAP nanoscaffolds were prepared in the wells as described above. Control wells without the SAPs had 60 μL of DMEM mixture and 40 μL of

PBS added. 100 μL of HaCaT cells (1.5×10^4 cells mL^{-1}) in DMEM mixture were seeded in each well on top of the various SAPs. The same was done for NIH/3T3 cells. The plates were left to incubate overnight (37°C/5% CO2). Three hours before each sampling (e.g. at t = −3 for the t = 0 sample), 60 μL of CellTiter 96® AQueous One Solution Cell Proliferation Assay (MTS; Promega) solution was added to every well of the plate for the particular time point. The plate was further incubated (37°C/5% CO_2) for three hours. At each sampling time point, the absorbance for the plate was read at 490 nm (BMG Labtech, FLUOstar OPTIMA).

Cell migration assay. SAP nanoscaffolds were prepared in the wells of specialized cell culture dishes (MatTek, glass bottom dish; 35 mm dish diameter, 10 mm glass; bottom, No. 1.5 glass thickness). These specialized dishes were manufactured with a glass coverslip at the bottom, enabling high-resolution light microscopy images of cells to be taken. Fibroblasts and keratinocytes were passaged and diluted to a cell density of 2.0×10^5 cells mL^{-1}. 100 μL of the cells were plated on top of the SAP nanoscaffolds and the dishes were topped up with an additional 3 mL of DMEM mixture. The dishes were placed in a microscope incubator (37°C/5% CO_2; Tokai Hit, Stage Top Incubator) and imaged with an inverted microscope (Olympus, IX81). Diffraction interference contrast (DIC) microscopy was performed on the samples over 12 hours at 10× magnification. Images were taken every 6 minutes. The total distances covered by the cells were tracked individually frame-by-frame using the 'Manual Tracking' plugin in Fiji[28]. Cells that migrated out of the frame or dividing during the recording were not tracked. A series of slices through the gel were taken and the optimal slice (i.e. most cells in focus) for each sample was chosen for the x-y- tracking. Cells that moved in the z-direction, through the slices, were not tracked.

1. Martin, P. Wound healing–aiming for perfect skin regeneration. *Science* **276**, 75–81 (1997).
2. Dersch, R., Steinhart, M., Boudriot, U., Greiner, A. & Wendorff, J. Nanoprocessing of polymers: applications in medicine, sensors, catalysis, photonics. *Polym Advan Technol* **16**, 276–282 (2005).
3. Gelain, F., Horii, A. & Zhang, S. Designer Self Assembling Peptide Scaffolds for 3 D Tissue Cell Cultures and Regenerative Medicine. *Macromol Biosci* **7**, 544–551 (2007).
4. Papini, R. ABC of burns - Management of burn injuries of various depths. *Brit Med J* **329**, 158–160, doi:10.1136/bmj.329.7458.158 (2004).
5. Atiyeh, B. S. & Costagliola, M. Cultured epithelial autograft (CEA) in burn treatment: three decades later. *Burns* **33**, 405–413 (2007).
6. Atiyeh, B. S., Gunn, S. W. & Hayek, S. N. State of the art in burn treatment. *World Journal of Surgery* **29**, 131–148 (2005).
7. Druecke, D. *et al.* Modulation of scar tissue formation using different dermal regeneration templates in the treatment of experimental full thickness wounds. *Wound repair and regeneration* **12**, 518–527 (2004).
8. Mac Neil, S. What role does the extracellular matrix serve in skin grafting and wound healing? *Burns* **20**, S67–S70 (1994).
9. Lee, J., Cuddihy, M. J. & Kotov, N. A. Three-dimensional cell culture matrices: state of the art. *Tissue Eng* **14**, 61–86 (2008).
10. Athanasiou, K. A., Niederauer, G. G. & Agrawal, C. Sterilization, toxicity, biocompatibility and clinical applications of polylactic acid/polyglycolic acid copolymers. *Biomaterials* **17**, 93–102 (1996).
11. Moran, J. M., Pazzano, D. & Bonassar, L. J. Characterization of polylactic acid-polyglycolic acid composites for cartilage tissue engineering. *Tissue Eng* **9**, 63–70 (2003).
12. Athanasiou, K., Schmitz, J. & Agrawal, C. The effects of porosity on in vitro degradation of polylactic acid-polyglycolic acid implants used in repair of articular cartilage. *Tissue Eng* **4**, 53–63 (1998).
13. Greenhalgh, D. G. The role of apoptosis in wound healing. *The international journal of biochemistry & cell biology* **30**, 1019–1030 (1998).
14. Yokoi, H., Kinoshita, T. & Zhang, S. Dynamic reassembly of peptide RADA16 nanofiber scaffold. *Proc Natl Acad Sci U S A* **102**, 8414–8419, doi:10.1073/pnas.0407843102 (2005).
15. Gelain, F., Horii, A. & Zhang, S. Designer Self-Assembling Peptide Scaffolds for 3-D Tissue Cell Cultures and Regenerative Medicine. *Macromol Biosci* **7**, 544–551 (2007).
16. Meng, H., Chen, L., Ye, Z., Wang, S. & Zhao, X. The effect of a self assembling peptide nanofiber scaffold (peptide) when used as a wound dressing for the treatment of deep second degree burns in rats. *J Biomed Mater Res B* **89**, 379–391 (2009).
17. Hauser, C. A. E. & Zhang, S. G. Designer self-assembling peptide nanofiber biological materials. *Chem Soc Rev* **39**, 2780–2790, doi:10.1039/b921448h (2010).
18. Wang, X. M., Horii, A. & Zhang, S. G. Designer functionalized self-assembling peptide nanofiber scaffolds for growth, migration, and tubulogenesis of human umbilical vein endothelial cells. *Soft Matter* **4**, 2388–2395, doi: Doi 10.1039/B807155a (2008).
19. Horii, A., Wang, X., Gelain, F. & Zhang, S. Biological designer self-assembling peptide nanofiber scaffolds significantly enhance osteoblast proliferation, differentiation and 3-D migration. *PloS one* **2**, e190 (2007).
20. Meng, H., Chen, L., Ye, Z., Wang, S. & Zhao, X. The effect of a self-assembling peptide nanofiber scaffold (peptide) when used as a wound dressing for the treatment of deep second degree burns in rats. *Journal of Biomedical Materials Research Part B: Applied Biomaterials* **89B**, 379–391, doi:10.1002/jbm.b.31226 (2009).
21. Abercrombie, M. & Heaysman, J. E. Observations on the social behaviour of cells in tissue culture. I. Speed of movement of chick heart fibroblasts in relation to their mutual contacts. *Exp Cell Res* **5**, 111–131 (1953).
22. Cory, G. in *Cell Migration* 25–30 (Springer, 2011).
23. Cai, G., Lian, J., Shapiro, S. S. & Beacham, D. A. Evaluation of endothelial cell migration with a novel in vitro assay system. *Methods in cell science: an official journal of the Society for In Vitro Biology* **22**, 107–114 (2000).
24. Chen, H.-C. in *Cell Migration* 15–22 (Springer, 2005).
25. Kraehenbuehl, T. P. *et al.* Three-dimensional extracellular matrix-directed cardioprogenitor differentiation: systematic modulation of a synthetic cell-responsive PEG-hydrogel. *Biomaterials* **29**, 2757–2766 (2008).
26. Kim, J. *et al.* Bone regeneration using hyaluronic acid-based hydrogel with bone morphogenic protein-2 and human mesenchymal stem cells. *Biomaterials* **28**, 1830–1837 (2007).
27. Ehrbar, M. *et al.* Elucidating the role of matrix stiffness in 3D cell migration and remodeling. *Biophysical Journal* **100**, 284–293 (2011).
28. Fiji Is Just ImageJ (2012).
29. Boland, E. D., Wnek, G. E., Simpson, D. G., Pawlowski, K. J. & Bowlin, G. L. Tailoring tissue engineering scaffolds using electrostatic processing techniques: a study of poly (glycolic acid) electrospinning. *J Macromol Sci Pure* **38**, 1231–1243 (2001).
30. Schulz III, J. T., Tompkins, R. G. & Burke, J. F. Artificial Skin. *Annu Rev Med* **51**, 231–244, doi: doi:10.1146/annurev.med.51.1.231 (2000).
31. Woodley, D. T., Wynn, K. C. & O'Keefe, E. J. Type IV collagen and fibronectin enhance human keratinocyte thymidine incorporation and spreading in the absence of soluble growth factors. *J Invest Dermatol* **94**, 139–143 (1990).
32. Alberts, B. *et al.* in *Molecular Biology of the Cell 4th edition* Ch. 19 (2002).
33. Hansbrough, J. F., Boyce, S. T., Cooper, M. L. & Foreman, T. J. Burn wound closure with cultured autologous keratinocytes and fibroblasts attached to a collagen-glycosaminoglycan substrate. *J Amer Med Assoc* **262**, 2125 (1989).
34. Clark, R. A. F., Folkvord, J. M. & Wertz, R. L. Fibronectin, as well as other extracellular matrix proteins, mediate human keratinocyte adherence. *J Invest Dermatol* **84**, 378–383 (1985).
35. Hynes, R. O. Integrins: versatility, modulation, and signaling in cell adhesion. *Cell* **69**, 11–25 (1992).
36. Witte, M. B. & Barbul, A. General principles of wound healing. *The Surgical clinics of North America* **77**, 509–528 (1997).
37. Izzard, C. S. & Lochner, L. R. Formation of cell-to-substrate contacts during fibroblast motility: an interference-reflexion study. *J Cell Sci* **42**, 81–116 (1980).
38. Steffensen, B., Häkkinen, L. & Larjava, H. Proteolytic events of wound-healing–coordinated interactions among matrix metalloproteinases (MMPs), integrins, and extracellular matrix molecules. *Crit Rev Oral Biol M* **12**, 373–398 (2001).
39. Ruoslahti, E. RGD and other recognition sequences for integrins. *Annu Rev Cell Dev Biol* **12**, 697–715, doi:10.1146/annurev.cellbio.12.1.697 (1996).
40. Woodley, D. T., Bachmann, P. M. & O'Keefe, E. J. Laminin inhibits human keratinocyte migration. *J Cell Physiol* **136**, 140–146, doi:10.1002/jcp.1041360118 (1988).
41. Nakamura, F. Biochemical, electron microscopic and immunohistological observations of cationic detergent-extracted cells: detection and improved preservation of microextensions and ultramicroextensions. *BMC Cell Biol* **2**, 10 (2001).
42. Buttke, T. M., McCubrey, J. A. & Owen, T. C. Use of an aqueous soluble tetrazolium/formazan assay to measure viability and proliferation of lymphokine-dependent cell lines. *J Immunol Methods* **157**, 233–240 (1993).
43. Malich, G., Markovic, B. & Winder, C. The sensitivity and specificity of the MTS tetrazolium assay for detecting the in vitro cytotoxicity of 20 chemicals using human cell lines. *Toxicology* **124**, 179–192 (1997).

Acknowledgments

The authors acknowledge the Australian Microscopy & Microanalysis Research Facility at the Centre for Microscopy, Characterization & Analysis, The University of Western Australia, funded by the University, State and Commonwealth Governments. Funding for this project comes from the Australian Research Council (ARC) Linkage Grant, Discovery Project & National Health and Medical Research Council (NHMRC) grants awarded to W/Prof. F. Wood and Dr. S. Iyer.

Author contributions

M.B. and D.H wrote the main manuscript text and performed all the experiments. M.W.F., F.M.W., F.G. and K.S.I. directed the experiments and contributed to the discussion of the results. All authors reviewed the manuscript and all authors have given approval to the final version of the manuscript.

Additional information

Supplementary information accompanies this paper at http://www.nature.com/scientificreports

Competing financial interests: The authors declare no competing financial interests.

How to cite this article: Bradshaw, M. *et al.* Designer self-assembling hydrogel scaffolds can impact skin cell proliferation and migration. *Sci. Rep.* **4**, 6903; DOI:10.1038/srep06903 (2014).

This work is licensed under a Creative Commons Attribution-NonCommercial-NoDerivs 4.0 International License. The images or other third party material in this article are included in the article's Creative Commons license, unless indicated otherwise in the credit line; if the material is not included under the Creative Commons license, users will need to obtain permission from the license holder in order to reproduce the material. To view a copy of this license, visit http://creativecommons.org/licenses/by-nc-nd/4.0/